Microstructure of J-band-forming cyanine dye monolayer probed by means of second-harmonic generation

Victor Mizrahi and G. I. Stegeman
Optical Sciences Center, University of Arizona, Tucson, Arizona 85721

Wolfgang Knoll
Max-Planck-Institut für Polymerforschung, Ackermannweg 10, D-6500 Mainz, Federal Republic of Germany
(Received 18 October 1988)

We have determined the microscopic symmetry of the J-band-forming amphiphatic cyanine dye (S120) to be C_2 by means of second-harmonic generation. We also demonstrate that the macroscopic distribution of the J aggregates is not isotropic, a result that facilitates our determination of the microscopic symmetry.

I. INTRODUCTION

In recent years second-harmonic generation (SHG) has gained popularity as a surface analytical technique.[1] In particular, numerous works have appeared where SHG was used to study monolayer or multilayer films of organic molecules deposited by the Langmuir-Blodgett (LB) deposition technique.[2–8] Often the interest is in determining the microscopic hyperpolarizability β of the individual molecules, and/or in determining the average tilt angle of amphiphilic molecules (i.e., molecules with one hydrophobic and one hydrophilic part) away from the substrate (or water surface) normal. This use of SHG generally rests on the key assumptions that, first, the second-order nonlinearity of an individual molecule, which is a third-rank tensor, is dominated by a single component, and second, that the molecules are all inclined close to some average angle to the substrate normal, with a random distribution of azimuthal angles.[2,3]

In this work we are also interested in determining the microstructure of an LB film by SHG, but our approach will of necessity be a different one. We are interested in monolayers of the J-band-forming amphiphatic cyanine dye, 1-methyl-1'-octadecyl-2,2'-cyanine iodide, also known as S120. This dye has been studied in monolayer form by a battery of techniques, including fluorescence microscopy and spectroscopy, electron microscopy and diffraction, and by synchrotron x-ray reflection.[9–11] It is known that in monolayer form, the molecules form into slightly elliptically shaped crystalline domains, known as J aggregates, of order 10 to 100 μm in diameter. Electron diffraction shows rotational symmetry, and a high degree of positional symmetry, within the aggregates, but an unambiguous determination of the crystal symmetry has not been achieved until now. However, a model for the microstructure, the so-called brickstone arrangement (which suggests that the lattice is arranged like a brick wall) is available.[12,13] In this work we will demonstrate, using SHG, that the J-aggregates have C_2 symmetry, in agreement with a generalized brickstone model.

Given what is known about these molecules, we are not prepared to assume that a single component of their microscopic hyperpolarizability is dominant, nor is this necessary for our purposes. Further, it will become evident from the data that the molecules were not isotropically distributed, a fact that we will use to our advantage.

We will begin, in Sec. II, with a more detailed discussion of the materials that we are studying, their preparation by the LB technique, and the brickstone model referred to earlier. In Sec. III we introduce the theory needed to understand how SHG may be used to determine the symmetry of the J aggregates. In Sec. IV we describe the SHG experimental apparatus used in this study. In Sec. V we present the experimental results and interpret them within the framework of the theory presented in Sec. II. Finally, in Sec. VI we summarize our conclusions.

II. MATERIALS

The cyanine dye (1-methyl-1'octadecyl-2,2'-cyanine iodide, S120) used in this study was synthesized by K.

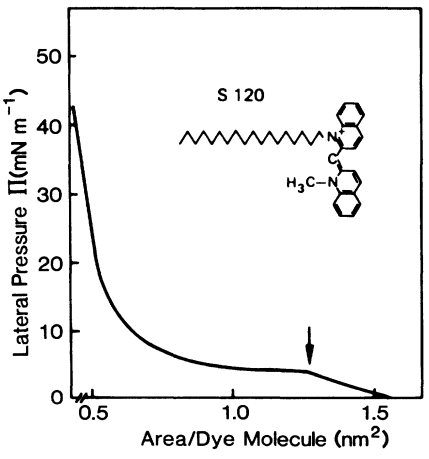

FIG. 1. Pressure-area isotherm of cyanine dye S120 (structure formula given in the inset) on pure H_2O (Millipore quality), pH of 5.5, $T=22$ °C. The arrow indicates the onset of the J-aggregate formation.

 ©1989 The American Physical Society

Wirthensohn. As shown in the inset of Fig. 1, this molecule is an amphipathic (surface-active) analog of the long-known pseudoisocyanine (1,1'-diethyl-2,2'cyanine), which was among the first systems to show Scheibe or J aggregation (i.e., red shift of the first electronic transition upon aggregation) in pure aqueous solutions.[14,15] By replacing one of the ethyl groups by a long alkyl chain (C_{18} in our case) these molecules now can be spread and organized as monomolecular layers at the water-air interface, but still retain their ability to form J aggregates.[16] The lateral pressure-induced formation of these (quasi-) two-dimensional crystallites can be seen in the pressure-area (Π-A) isotherms by the onset of a first-order phase transition (see arrow in Fig. 1) and can be also be controlled microscopically: the high fluorescence quantum yield of the aggregates allows one to observe the growing crystallites by fluorescence microscopy.[9] An example of their typical ellipsoidal shapes and the size distribution, with diameters of up to 100 μm, is given in Fig. 2. The picture was taken with polarized excitation light. The fluorescence emission from each crystallite has a homogeneous intensity, which depends on the relative orientation of the transition dipole moment of the aggregates and the electric field, and has a unique polarization.[9] This optical evidence for the single-crystalline character of each aggregate was further confirmed by electron-diffraction studies.[11] The diffraction-spot pattern obtained from monolayers was compatible with the brickstone arrangement proposed by Kuhn and coworkers,[12,13] assuming in addition that two chromophores constitute the unit cell of the crystal lattice [schematically depicted in Fig. 3(a)].

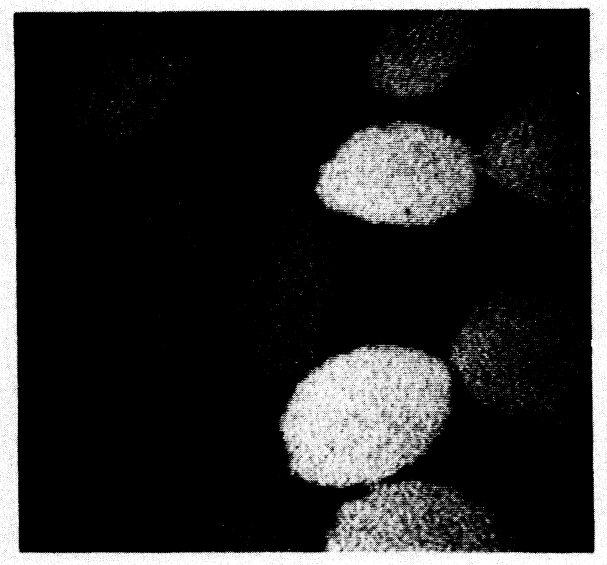

FIG. 2. Fluorescence microscopic picture of S120 aggregates taken directly at the water surface. The area shown corresponds to 100×100 μm^2. Lateral pressure $\Pi=15$ mN/m. Excitation is with polarized light, hence only crystallites with their transition dipole moment parallel to the electric field fluoresce brightly.

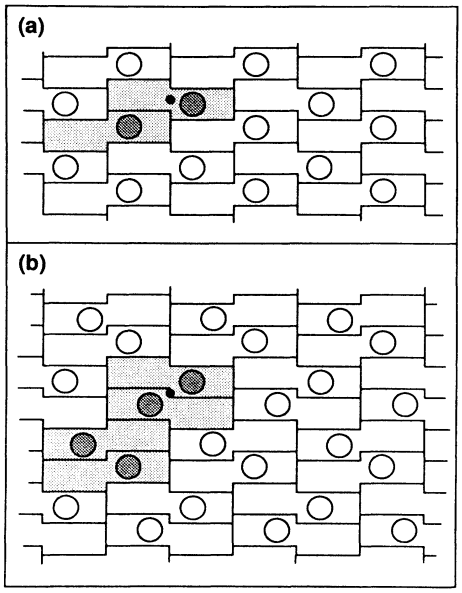

FIG. 3. Schematic arrangement of the S120 chromophore heads in the J aggregates as deduced from SHG and electron diffraction. Drawn is a top view looking down on the water surface. The chinolin rings are presumed to be essentially perpendicular to the substrate, but with a twist relative to each other along the connecting C atom (see Fig. 1). In this block schematic we show the projection of the rings on the surface. The circles indicate the positions of the octadecyl chain tail groups. Typical dimensions of the blocklike projections are 15.4×3.6 Å^2. In (a) we show a conventional Brickstone model with two molecules per unit cell (shaded blocks). This has C_2 symmetry only if we ignore the tails. In (b) we show a "double brickstone" model, with four molecules per unit cell and exact C_2 symmetry. One center of rotation symmetry has been indicated by a heavy dot in each case. In both (a) and (b), equal numbers of molecules with a right- and a left-hand twist are used.

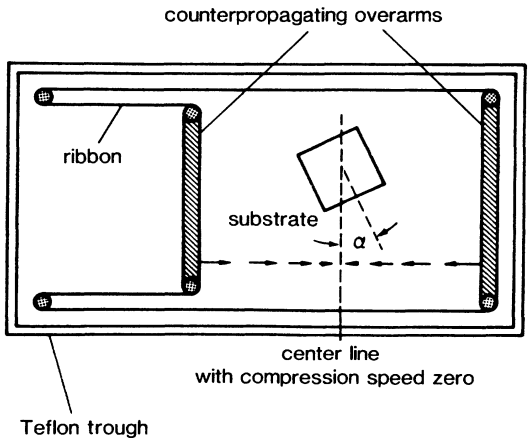

FIG. 4. Schematic drawing of the Langmuir trough used for the preparation of the S120 monolayers. Shown are the two counterpropagating overarms that compress the spread molecules and induce a compression speed profile as indicated by the arrows. The center line where the dipping of the substrate occurs remains still. For the (near-) horizontal transfer of the S120 aggregate layer, an arbitrary angle α between the orientation of the substrate and the center line could be chosen.

In summary, a monomolecular layer of S120 compressed on a pure water subphase to a lateral pressure of $\Pi = 40$ mN m^{-4} (corresponding to an area per molecule of about $A = 0.55$ nm^2), is composed of densely packed two-dimensional single crystals of slightly elliptical shape with diameters from 10 to 100 μm.

Our monolayers were prepared using two different Langmuir troughs. For our SHG studies we used the Joyce-Loebl tank equipped with a Wilhelmi plate and microbalance. A special feature of this system is the half-immersed Teflon-coated glass-fiber ribbon that confines the spread molecules to a well-defined area with a constant perimeter. Compression is achieved by two counterpropagating overarms so that in the center of the working area where the monolayer transfer occurs, a line of zero relative compression spread is maintained (see Fig. 4). As discussed below and elsewhere,[17] we believe that this is a crucial point for a reproducible orientation distribution of anisotropically shaped crystallites.

The other Langmuir trough used is homebuilt, operating with a single movable barrier. Surface pressure readings are taken also with a Wilhelmi system. Integrated into the bottom of this trough is a microscope objective that allows for the fluorescence microscopic observation of the dye aggregation.[18]

Transfer of the monolayers onto hydrophobic substrates was performed in the following way. First, two clean BK-7 Schott glass slides ($1 \times 1 \times \frac{1}{16}$ in.) were mounted together. The edges were sealed with Teflon ribbon to prevent the subphase liquid from penetrating between the two glass plates. This assembly was then coated with one cadmium arachidate monolayer by the usual vertical dipping technique. Dye monolayer transfer onto the front side was subsequently performed on the down stroke by hand, with the substrate being mounted nearly horizontally. The angle α between an arbitrarily chosen axis in the plane of the substrate and the center line of the monolayer could be chosen freely (see Fig. 4) to an accuracy of $\pm 5°$. While submerged, the substrate was rotated to the vertical and the water surface aspirated. A protective overlayer of arachidic acid was added in a conventional upstroke. Finally, the two slides were separated and only the front one was used for the experiments. This procedure ensured the coating of only one side of the substrate with the back side being absolutely free of contamination.

Prior to the SHG experiments, linear absorption spectra were taken to test the successful formation and transfer of S120 J aggregates. A typical example is shown in Fig. 5.

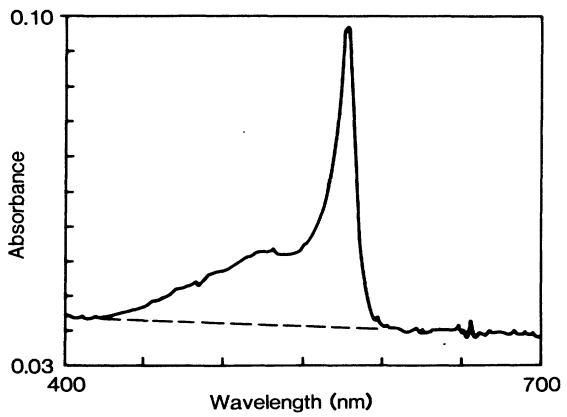

FIG. 5. Typical absorption spectrum of an S120 aggregate monolayer (not corrected for substrate contributions).

III. THEORY

To determine the symmetry of the sample with second-harmonic generation (SHG), it is necessary to understand the tensorial nature of SHG as it applies to a monolayer of $\chi^{(2)}$ active molecules. In what follows, we are interested *only* in the symmetry properties of SHG, and hence ignore all Fresnel, geometrical, and additional factors that must be considered to properly calculate the absolute SHG signal from a given sample. A more complete treatment may be found in Ref. 19.

The geometry of a SHG experiment is illustrated in Fig. 6. We adhere to the coordinate system and notation of Ref. 19. In the transmission experiment the laser, oscillating at frequency ω, is incident at angle θ on the glass substrate, with the Langmuir-Blodgett (LB) film on the second surface of the glass. The second harmonic at frequency 2ω, which is generated by the film, travels collinearly with the laser beam, and is detected in the forward direction. Details of the experimental SHG system are given in Sec. IV.

The Cartesian coordinate system, in the reference frame of the LB film, is oriented so that $\hat{z}$ points perpendicular to the film away from the substrate, and $\hat{y}$ points along any preferred direction in the plane of the film.

For this work, we will only be concerned with a linearly polarized laser, and with detecting a given linear component of the second harmonic. The angle γ describes

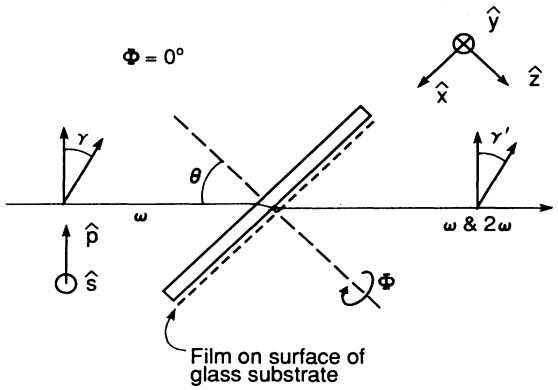

FIG. 6. Substrate-based coordinate system used in determining the polarization and angular orientation properties of SHG from the LB film. The film is on the second surface of the glass substrate, as indicated by the dashed line. The $\Phi = 0°$ case is shown. For $\Phi = 0°$, we have $\hat{s} \| -\hat{y}$. γ and γ' denote the polarization of the fundamental at ω, and the second-harmonic at 2ω, respectively. For $\gamma = 0$ the light is $\hat{p}$ polarized, and for $\gamma = 90°$ it is $\hat{s}$ polarized.

the direction of the laser beam electric field, as illustrated in Fig. 6. For $\gamma=0°$, the laser is $\hat{\mathbf{p}}$ polarized; for $\gamma=90°$, the laser is $\hat{\mathbf{s}}$ polarized. Similarly, γ' describes the direction of the selected 2ω polarization. The orientation of the film about the axis normal to the substrate is described by the angle Φ, where $\Phi=0°$ corresponds to $\hat{\mathbf{y}}=-\hat{\mathbf{s}}$ for any θ.

Now let us first consider the SHG signal from a single oriented J aggregate, whose preferred direction, if any, points along $+\hat{\mathbf{y}}$. (Clearly if the J aggregate were isotropic in the plane of the film, then the choice of $\hat{\mathbf{y}}$ would be arbitrary.) Ignoring all Fresnel factors, we have, for a unit-magnitude laser electric field at the film,

$$\begin{aligned}\mathbf{E}_\omega(\gamma,\theta,\Phi)&=(\sin\gamma)\hat{\mathbf{s}}+(\cos\gamma)\hat{\mathbf{p}}\\&=-(\sin\gamma\sin\Phi+\cos\gamma\cos\theta\cos\Phi)\hat{\mathbf{x}}\\&\quad+(\cos\gamma\cos\theta\sin\Phi-\sin\gamma\cos\Phi)\hat{\mathbf{y}}\\&\quad-(\cos\gamma\sin\theta)\hat{\mathbf{z}}\ .\end{aligned}\tag{3.1}$$

For a given nonlinear susceptibility tensor $\boldsymbol{\chi}^{(2)}$, whose form depends on the symmetry of the J aggregate, we may write the nonlinear polarization vector $\mathbf{P}_{2\omega}$,

$$\mathbf{P}_{2\omega}=\boldsymbol{\chi}^{(2)}:\mathbf{E}_\omega\mathbf{E}_\omega\ .\tag{3.2}$$

This oscillating polarization generates a propagating second-harmonic electric field $\mathbf{E}_{2\omega}$. As we are not interested in calculating actual signal levels here, but are only interested in the polarization properties of the second harmonic, and whether or not it can exist for a given γ,θ,Φ, we write simply, ignoring overall constants of proportionality,

$$\begin{aligned}\mathbf{E}_{2\omega}(\gamma,\theta,\Phi)&=(\mathbf{P}_{2\omega}\cdot\hat{\mathbf{s}})\hat{\mathbf{s}}+(\mathbf{P}_{2\omega}\cdot\hat{\mathbf{p}})\hat{\mathbf{p}}\\&=-(P_x\sin\Phi+P_y\cos\Phi)\hat{\mathbf{s}}\\&\quad+(-P_x\cos\theta\cos\Phi\\&\quad+P_y\cos\theta\sin\Phi-P_z\sin\theta)\hat{\mathbf{p}}\ .\end{aligned}\tag{3.3}$$

Finally, we denote the total second-harmonic signal (as, for example, measured by the total number of 2ω photons generated per laser pulse) by $S(\gamma,\gamma',\theta,\Phi)$, where we detect only the second harmonic polarized at the angle γ' (see Fig. 6). In this case we have

$$\begin{aligned}S(\gamma,\gamma',\theta,\Phi)=|&[\mathbf{E}_{2\omega}(\gamma,\theta,\Phi)\cdot\hat{\mathbf{s}}]\sin\gamma'\\&+[\mathbf{E}_{2\omega}(\gamma,\theta,\Phi)\cdot\hat{\mathbf{p}}]\cos\gamma'|^2\ ,\end{aligned}\tag{3.4}$$

again ignoring overall constants of proportionality. Our principal interest in Eq. (3.4) is that we can use it to predict the form of the Φ dependence of the SHG signal. Ignoring anisotropy in the linear optical properties of the monolayer, the essential information is contained in the $\boldsymbol{\chi}^{(2)}$, whose form depends on the crystal symmetry of the J aggregate.

The generalization to the case of a macroscopic distribution of J aggregates, each of which is assumed to have its preferred direction oriented at some angle Φ_1 with respect to the $\hat{\mathbf{y}}$ axis of the film as a whole, is straightforward. (Again, if the macroscopic distribution of aggregates is isotropic, then the choice of $\hat{\mathbf{y}}$ is arbitrary.) Since the individual aggregates are relatively large (10–100 μm diameter) as compared with the second-harmonic wavelength (0.5 μm), we average the total signal from each individual aggregate[2] over the macroscopic distribution function $\rho(\Phi_1)$. Here $\rho(\Phi_1)$ gives the number of aggregates oriented at Φ_1, per unit Φ_1. So now the total second-harmonic signal is given by

$$S(\Phi)=\int_0^{2\pi}\rho(\Phi_1)S^{\mathrm{mic}}(\Phi-\Phi_1)d\Phi_1\ ,\tag{3.5}$$

where $S^{\mathrm{mic}}(\Phi-\Phi_1)$ is the second-harmonic signal from an individual microscopic aggregate, oriented at $\Phi-\Phi_1$ relative to the laboratory frame $\Phi=0$ axis, and where we have suppressed the γ,γ',θ arguments here.

Now the distribution function can always be expanded in a Fourier series

$$\rho(\Phi_1)=\sum_{m=0}^{\infty}\rho_m\cos(m\Phi_1+\delta_m)\tag{3.6}$$

where the ρ_m and δ_m determine the macroscopic distribution. We will see in Sec. V that $\rho(\Phi_1)$ can be sufficiently well determined for our purposes by measuring $S(\Phi)$.

For a given $\boldsymbol{\chi}^{(2)}$, θ, γ, and γ', $S^{\mathrm{mic}}(\Phi-\Phi_1)$ can similarly be expanded in a Fourier series

$$S^{\mathrm{mic}}(\Phi-\Phi_1)=\sum_{n=0}^{\infty}S_n\cos[n(\Phi-\Phi_1)+\epsilon_n]\ .\tag{3.7}$$

In fact, for any given symmetry class associated with the J aggregate, only a small number of terms in this series completely specify $S^{\mathrm{mic}}(\Phi-\Phi_1)$. Since cosine functions of different frequencies are orthogonal, even fewer terms generally survive the integration of Eq. (3.5) to contribute to $S(\Phi)$. Even so, we will see in Sec. V that it is possible to determine the microscopic symmetry class of the individual J aggregate in this case, even though the laser beam samples a distribution of J aggregates.

Substituting Eqs. (3.6) and (3.7) into Eq. (3.5), and performing the integration, we have

$$S(\Phi)=\pi\rho_0S_0+\pi\sum_{m=0}^{\infty}\rho_mS_m\cos(m\Phi+\delta_m+\epsilon_m)\ ,\tag{3.8}$$

where we have, without loss of generality, set $\delta_0=\epsilon_0=0$. It is important to note that the macroscopic SHG signal $S(\Phi)$ will show an angular dependence containing only those frequencies which are present both in the microscopic signal $S^{\mathrm{mic}}(\Phi)$, *and* in the macroscopic distribution function $\rho(\Phi)$. Hence the more isotropic is $\rho(\Phi)$, the less information about $S^{\mathrm{mic}}(\Phi-\Phi_1)$ is present in $S(\Phi)$.

The nonvanishing components of $\boldsymbol{\chi}^{(2)}$, and any relationships between them, for the various possible symmetry classes, have been conveniently tabulated in Ref. 20. For any given symmetry class, one can use this information about the form of $\boldsymbol{\chi}^{(2)}$, together with Eqs. (3.1)–(3.4), to make specific predictions about the polarization properties of the SHG expected from any given oriented J aggregate. Further, given the macroscopic distribution function $\rho(\Phi_1)$, together with Eq. (3.8), one can predict

the Φ dependence of the SHG signal from a collection of J aggregates, for any given microscopic symmetry class of the individual J aggregates. In Sec. V we will see that it will, in fact, be possible to work backwards, given the results of our experiments on this material, to obtain microscopic information on the nature of the J aggregates. First we turn to a description of the SHG experimental system used to take the data.

IV. EXPERIMENTAL PROCEDURE

The SHG experimental apparatus is illustrated schematically in Fig. 7. The LB film to be studied, deposited on one side of a 1-in.^{2} square by $\frac{1}{16}$-in.-thick (25.4×25.4×1.6 mm) BK-7 Schott glass substrate, is mounted on computer-controlled rotational stages, with angular degrees of freedom as shown. The laser beam passes through the center of the sample from the substrate side (LB film on second surface), which is adjusted so that the beam intersects a fixed spot on the film when the substrate is rotated. The laser beam consists of 35-ps pulses, at 10 pulses per sec, at a wavelength of 1.064 μm. Typical pulse energies of 1 mJ at the sample were used in the experiments described here. The laser beam was collimated with a telescope to have a measured diameter (at the $1/e^2$ points) of 2.3 mm, thus illuminating a large section of the sample, including of order 10^3 J aggregates.

To eliminate detection of any second harmonic not generated by the sample or substrate, the sample is placed immediately after a long-wavelength pass (LWP) filter, which passes the laser but blocks any second harmonic, and immediately before a short-wavelength pass (SWP) filter, which passes the second harmonic from the sample but blocks most of the laser beam. As these glass filters are isotropic, and have been carefully mounted at near-normal incidence to the laser beam, they do not contribute to the detected second-harmonic signal.[19] For the nonnormal incidence measurements described below ($\theta > 0°$), the glass substrate has, by itself, a surface second-harmonic signal that is more than two orders of magnitude smaller than the peak signals observed from the LB film. Even so, because of an interference between the substrate and the film contribution, this can, for the weaker signals, cause a modulation of order 10% of the detected signal, if plotted as a function of the angle of incidence θ of the laser beam on the substrate. Since the glass substrate is demonstrably isotropic, these Maker fringes will have no effect on our interpretation of the symmetry properties of the LB films, as discussed below.

The residual laser beam, after the first SWP filter, is eliminated by the use of dichroic mirrors, a narrow-band [2.8-nm full width at half maximum (FWHM)] interference filter, centered at 0.532 μm, and additional SWP filters. The high-gain ($\sim 10^8$), end-on, photon-counting photomultiplier tube (PMT) used to detect the second harmonic does not respond at 1.064 μm. The use of a narrow-band filter, coupled with a deliberately small acceptance angle for the detector ($\pm 0.2°$), serves to discriminate against any two-photon-induced fluorescence from the sample. Such fluorescence was not a problem here, as evidenced by the lack of signal when the sample was at normal incidence ($\theta = 0°$) to the laser. This background count rate was less than one detected SHG photon per 1000 laser shots. At $\theta = 0°$, any fluorescence would continue to be allowed, but SHG is forbidden by symmetry (see discussion below). Nonetheless, a 0.3-m grating spectrometer was used to verify that the signal was spectrally pure, and at the second-harmonic wavelength. Filters were generally used, so the detection system was polarization insensitive, and also easier to align. In these experiments, typical signal levels were of the order of one second-harmonic photon detected out of $\sim 10^{15}$ laser photons per laser shot.

A well-defined polarization state of the laser was select-

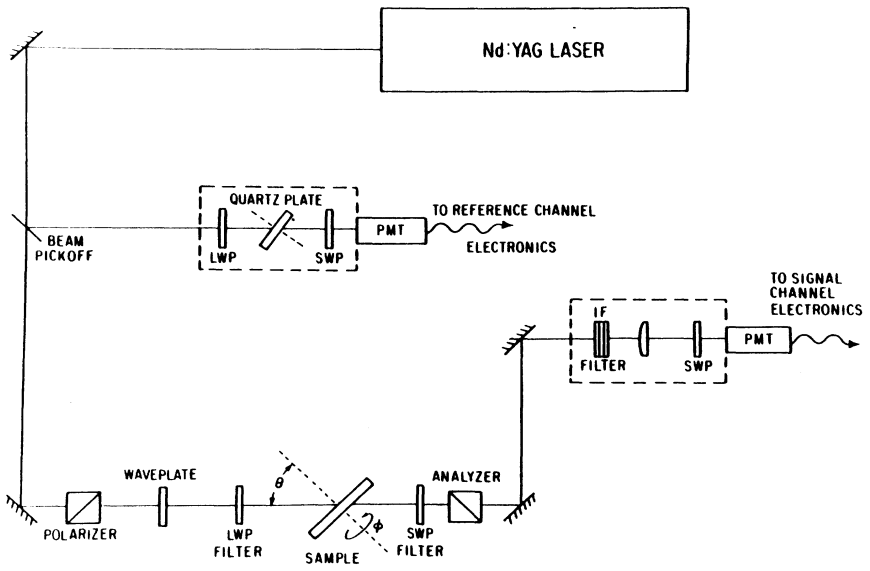

FIG. 7. SHG experimental apparatus, as described in Sec. IV of the text.

ed with a Glan-laser prism polarizer, followed by a quartz half-wave plate. A particular polarization state of the second harmonic was selected by a similar polarizer serving as an analyzer.

To deal with the laser pulse amplitude and pulse length fluctuations, about 5% of the laser beam is picked off with a beam splitter and sent to a separate reference channel. The reference channel uses a crystal quartz plate for SHG, which is detected by a PMT selected and wired for high linearity. The output of both the signal and reference channel PMT's is sent to separate boxcar integrators, the outputs of which are digitized and sent to the data acquisition computer. The computer performs a shot-by-shot normalization of the signal-channel output to the reference-channel output, controls the sample rotation stages, and stores and processes the data. The SHG experimental system has been tested for systematic errors at the 5% level of confidence.[21]

V. RESULTS AND INTERPRETATION

A second-harmonic signal was observed from the S120 sample, prepared as explained in Sec. II. To gain information about the macroscopic symmetry of the sample, the Φ dependence of the signal was observed under $\hat{p}_{in} \rightarrow \hat{p}_{out}$ conditions, by which we mean that the incident laser beam was $\hat{p}$ polarized, and the analyzer was set to select the $\hat{p}$-polarized second-harmonic output. The results of this Φ scan are shown in Fig. 8, taken with $\theta = 35°$. The $\Phi = 0° - 180°$ axis corresponds, for $\alpha = 0°$, to this axis being parallel to the center line of the monolayer on the surface of the Langmuir trough during the horizontal dipping. (α is measured between the $-\hat{y}$ axis of the substrate and this center line; see Figs. 4 and 6.) Clearly the sample is not macroscopically isotropic, but instead shows an approximate twofold rotational symmetry about the $\hat{z}$ axis. This result is somewhat surprising, as it has generally been believed that molecules on the water surface of a Langmuir trough are isotropically distributed. In fact, during the isothermal compression stage, a force is applied to the molecules from two counterpropagating overarms moving along one axis of the water surface (see Fig. 4). Since the aggregates are slightly ellipsoidal in shape (see Fig. 2), it is possible that some orientation of these ellipses occurs during this compression. To test this, we deposited another film on a similar substrate, as described in Sec. II, but this time with the substrate rotated to approximately $\alpha = 45°$ in the plane of the water surface (horizontal dipping is employed throughout) so that the compression axis was rotated by 45° relative to the marked edge of the substrate. The SHG measurements of this film are shown in Fig. 9. As expected for our interpretation, the origin of the curve is shifted. The direction of the shift is correct. The magni-

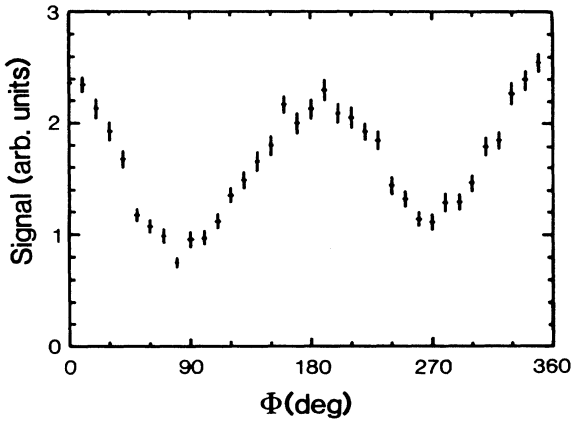

FIG. 8. Measured second-harmonic signal as a function of substrate orientation angle Φ for the S120 sample. The laser is $\hat{p}$ polarized, the analyzer is set to detect the $\hat{p}$-polarized second harmonic, and $\theta = 35°$ in this experiment. Each data point is an average of 100 laser shots, with the error bars indicating the standard error of the mean. Note the twofold rotational symmetry in the data.

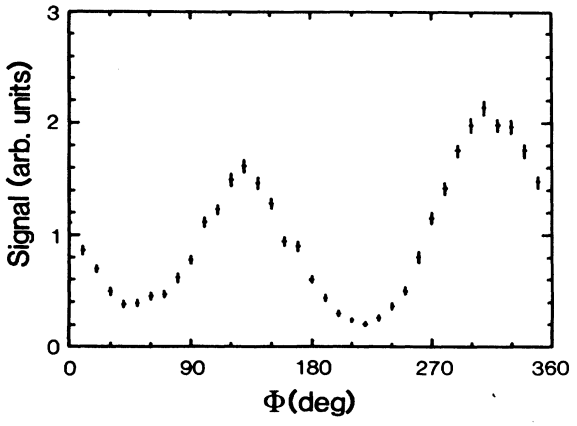

FIG. 9. As in Fig. 8, but this sample was rotated approximately 45° during the horizontal dipping procedure (see Fig. 4). The corresponding phase shift suggests that there is some preferred orientation of the J aggregates on the water surface.

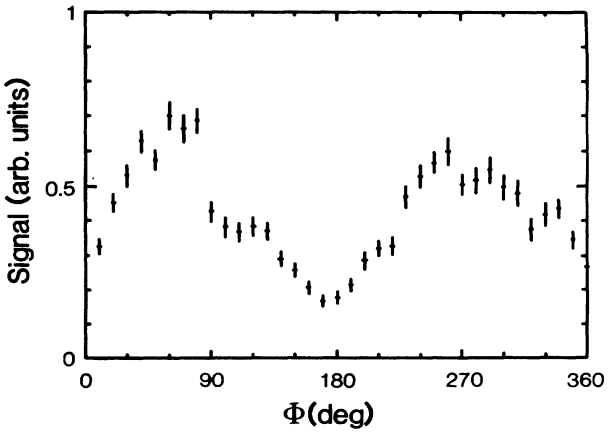

FIG. 10. As in Fig. 8, the same sample was used, but here the analyzer was set to detect $\hat{s}$-polarized light. The laser was still $\hat{p}$ polarized. The SHG signal shows twofold rotational symmetry, ruling out C_{2v}, C_4, or C_6 symmetry for a single J aggregate, as explained in the text.

tude of the shift is only approximately 45° as the deposition was done by hand. Nonetheless, this is convincing evidence.

This twofold symmetry in the distribution of the J aggregates is fortuitous, as it allows for the unambiguous determination of the microscopic symmetry of a single J aggregate. We will show this below.

First, we consider some of the polarization properties of the SHG. There exists a clear $\hat{\mathbf{p}}_{\text{in}} \rightarrow \hat{\mathbf{s}}_{\text{out}}$ signal from these samples. Given the nonzero $\chi^{(2)}$ elements for each symmetry class, taken from Ref. 20, together with Eqs. (3.1)–(3.4) for the second-harmonic signal from any given oriented J aggregate, it is straightforward to show that there could not be a $\hat{\mathbf{p}}_{\text{in}} \rightarrow \hat{\mathbf{s}}_{\text{out}}$ signal from a single J aggregate if it possessed C_{4v}, C_{6v}, or isotropic microscopic symmetry. This conclusion is in no way altered by averaging over the macroscopic distribution, as given by Eq. (3.5).

Further, there is no significant $\hat{\mathbf{s}}_{\text{in}} \rightarrow \hat{\mathbf{s}}_{\text{out}}$ signal. The same line of reasoning shows that such a signal could only come about if the microscopic symmetry of a single J aggregate were C_1 (i.e., no symmetry), C_{1v}, C_3, or C_{3v}. We therefore exclude these from consideration. Precisely the same conclusion is reached by noting, as in Sec. IV, that there is no significant normal incidence ($\theta = 0°$) signal for these samples for any combination of polarization components.

Now let us consider the possibility that a J aggregate has a microscopic C_4 or C_6 symmetry. The observed polarization properties do not exclude this possibility. Using Eqs. (3.1)–(3.4) of Sec. III, it is straightforward to show that the SHG signal from a single aggregate with either C_4, or C_6 microscopic symmetry would be constant during a Φ scan (i.e., $S_m = 0$ for $m > 0$). Therefore, from Eq. (3.8) we see that the macroscopic SHG signal $S(\Phi)$ would also be a constant function of Φ, in clear contradiction to our data, as shown in Fig. 8.

Finally, we are left with the possibility that a J aggregate has either C_2 or C_{2v} symmetry. Again, from Eqs. (3.1)–(3.4), it is straightforward to show that the SHG signal from a single aggregate, for the special case of $\hat{\mathbf{p}}_{\text{in}} \rightarrow \hat{\mathbf{s}}_{\text{out}}$, would show fourfold symmetry during a Φ scan if the J aggregate was C_{2v}, but would show twofold symmetry if the aggregate was C_2. But since we have seen that the macroscopic distribution of J aggregates has twofold symmetry as a function of Φ, we can specialize the form of $S(\Phi)$, given in Eq. (3.8), to

$$S(\Phi) = \pi \rho_0 S_0 + \pi \sum_{m=0}^{\infty} \rho_{2m} S_{2m} \cos(2m\Phi + \delta_{2m} + \epsilon_{2m}) \, . \tag{5.1}$$

Because of the anisotropy in the macroscopic distribution function, the macroscopic signal $S(\Phi)$ would show twofold symmetry if the aggregates are C_2, and fourfold symmetry (or isotropy if $\rho_4 \ll \rho_0$) if the aggregates are C_{2v}. In Fig. 10 we present the results of a $\hat{\mathbf{p}}_{\text{in}} \rightarrow \hat{\mathbf{s}}_{\text{out}}$ Φ scan. The twofold symmetry is evident, and a single J aggregate therefore has C_2 symmetry. This represents the first actual determination of the microscopic symmetry class of a single J aggregate.

C_2 symmetry is consistent with a conventional brickstone model. If we also consider the electron diffraction results that suggest that there are two "bricks" per unit cell,[11] and take into account packing considerations, we are led to a specific configuration sketched in Fig. 3(a). One drawback of this picture is that we must assume that the SHG measurements are not sensitive to the position of the octadecyl chain tails. This may be, but as an alternative we have sketched in Fig. 3(b) what we will refer to as a "double brickstone model." This arrangement has exact C_2 symmetry, even considering the tails. It is also consistent with the electron diffraction results. The red shift upon J aggregation will be less in this arrangement than in the conventional brickstone. Another testable difference between these two pictures is that the aggregates in the double brickstone have no permanent dipole moment, whereas the arrangement in Fig. 3(a) does. We intend to pursue this in future work.

It is interesting to note that had the macroscopic distribution of J aggregates been isotropic, it would not have been possible to reason as we have in distinguishing between C_2, C_{2v}, C_4, and C_6 symmetry for a single J aggregate, necessitating an experiment on a single J aggregate with a tightly focused laser beam and highly precise positioning of the sample. Greater symmetry in the macroscopic distribution means greater loss of information, relative to a single oriented J aggregate.

Fortunately, enough information was retained in a distribution with twofold symmetry to be useful. This suggests the possibility of deliberately introducing some partial orientation into an otherwise isotropic distribution of molecules to enhance the information content.

VI. CONCLUSION

We have deduced that the microscopic symmetry of a single J aggregate of amphiphatic cyanine dye, deposited by the Langmuir-Blodgett technique, is C_2 symmetry. We have done this using a combination of the polarization properties and angular dependence of the second-harmonic signals of these $\chi^{(2)}$-active molecules.

The approach that we have used should be applicable to other systems of interest. Although a complete determination of the microscopic symmetry of a single J aggregate, in a distribution of J aggregates, relied on the fortuitous result that the macroscopic distribution function was not isotropic, it may be possible to deliberately introduce anisotropy into otherwise isotropic LB films. Such a strategy has been successful in using SHG to study the columnar growth microstructure of inorganic thin films.[22] Finally, we have conclusively demonstrated that the inherent preferred direction on the water surface of a Langmuir-Blodgett deposition trough can, in some circumstances, lead to significant ordering of the molecules, observable by second-harmonic generation.

ACKNOWLEDGMENTS

This research was supported by U.S. Air Force Office of Scientific Research Contract No. AFOSR-87-0344 and the Joint Services Optical Program Contract No. F49620-88-C-0009. We wish to thank Dr. V. Enkelmann of the Max-Planck-Institut für Polymerforschung for help in interpreting the electron diffraction results.

[1]Y. R. Shen, J. Vac. Sci. Technol. B **3**, 1464 (1985), and references therein.

[2]J. R. Girling, N. A. Cade, P. V. Kolinsky, J. D. Earls, G. H. Cross, and I. R. Peterson, Thin Solid Films **132**, 101 (1985).

[3]Th. Rasing, Y. R. Shen, M. W. Kim, P. Valint, Jr., and J. Bock, Phys. Rev. A **31**, 537 (1985).

[4]Th. Rasing, Y. R. Shen, M. W. Kim, and S. Grubb, Phys. Rev. Lett. **55**, 2903 (1985).

[5]Th. Rasing, G. Berkovic, Y. R. Shen, S. G. Grubb, and M. W. Kim, Chem. Phys. Lett. **130**, 1 (1986).

[6]G. Berkovic, Th. Rasing, and Y. R. Shen, J. Opt. Soc. Am. B **4**, 945 (1987).

[7]I. R. Girling, N. A. Cade, P. V. Kolinsky, R. J. Jones, I. R. Peterson, M. M. Ahmad, D. B. Neal, M. C. Petty, G. G. Roberts, and W. J. Feast, J. Opt. Soc. Am. B **4**, 950 (1987).

[8]G. Berkovic, R. Superfine, P. Guyot-Sionnest, Y. R. Shen, and P. N. Prasad, J. Opt. Soc. Am. B **5**, 668 (1988).

[9]C. Duschl, M. Lösche, A. Miller, A. Fischer, H. Möhwald, and W. Knoll, Thin Solid Films **133**, 65 (1985).

[10]C. Duschl, W. Frey, C. Helm, J. Als-Nielsen, H. Möhwald, and W. Knoll, Thin Solid Films **159**, 386 (1988).

[11]Claus Duschl, Wolfgang Frey, and Wolfgang Knoll, Thin Solid Films **160**, 251 (1988).

[12]V. Czikkely, H. D. Försterling, and H. Kuhn, Chem. Phys. Lett. **6**, 11 (1970).

[13]H. Bücher and H. Kuhn, Chem. Phys. Lett. **6**, 183 (1970).

[14]E. E. Jelley, Nature **139**, 631 (1937).

[15]G. Scheibe, Kolloid Z. **82**, 1 (1938).

[16]H. Kuhn, D. Möbius, and H. Bücher, in *Physical Methods of Chemistry,* edited by A. Weissberger and B. Rossiter (Wiley-Interscience, New York, 1972), Vol. 1.

[17]Victor Mizrahi, G. I. Stegeman, and W. Knoll, Chem. Phys. Lett. (to be published).

[18]M. Lösche and H. Möhwald, Rev. Sci. Instrum. **55**, 1968 (1984).

[19]Victor Mizrahi and J. E. Sipe, J. Opt. Soc. Am. B **5**, 660 (1988). Note that in Eq. (3.33) the $\epsilon(2\omega)$ should have been $\epsilon'(2\omega)$.

[20]P. Guyot-Sionnest, W. Chen, and Y. R. Shen, Phys. Rev. B **33**, 8254 (1986).

[21]J. E. Sipe, Victor Mizrahi, and G. I. Stegeman, Phys. Rev. B **35**, 9091 (1987).

[22]Victor Mizrahi, F. Suits, J. E. Sipe, U. J. Gibson, and G. I. Stegeman, Appl. Phys. Lett. **51**, 427 (1987).

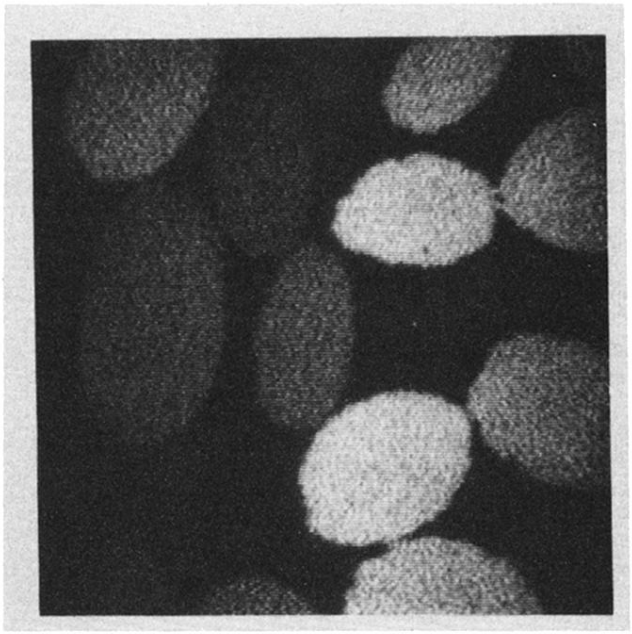

FIG. 2. Fluorescence microscopic picture of S120 aggregates taken directly at the water surface. The area shown corresponds to $100 \times 100\ \mu m^2$. Lateral pressure $\Pi = 15$ mN/m. Excitation is with polarized light, hence only crystallites with their transition dipole moment parallel to the electric field fluoresce brightly.